Electronic supplementary information (ESI) for

Coordination polymers with salicylaldehyde ligand: Structural diversity, selective sorption and luminescent sensing property

Yi Liu, Yue Zhao, Zhi-Qiang Liu, Xiao-Hui Liu, Xiu-Du Zhang and Wei-Yin Sun*

Coordination Chemistry Institute, State Key Laboratory of Coordination Chemistry, School of Chemistry and Chemical Engineering, Nanjing National Laboratory of Microstructures, Collaborative Innovation Center of Advanced Microstructures, Nanjing University, Nanjing 210023, China

*Corresponding author.

Email address: sunwy@nju.edu.cn (W. Y. Sun).

Experimental

Single crystal X-ray diffraction. Crystallographic data for **1** - **5** were collected on a Bruker Smart Apex II CCD single-crystal X-ray diffractometer with a graphite-monochromated Mo Kα radiation (λ = 0.71073 Å). The integration of the diffraction data and the intensity corrections for the Lorentz and polarization effects were carried out using the SAINT program.[S1] Absorption corrections were carried out using SADABS.[S2] Structures were solved by direct methods and refined by the full-matrix least-squares method using the SHELXL-2018 program of the SHELXTL package.[S3] All non-hydrogen atoms were refined on F^2 anisotropically. The hydrogen atoms were calculated geometrically and refined isotropically using the riding model. The solvent molecules in the unit cell have been taken into account with the SQUEEZE option of the PLATON program.[S4] The formula of **1**-**3** was calculated based on volume/count electron analysis, TG and elemental analysis. The reported refinements are of the guest-free structures obtained by the SQUEEZE routine, and the results are attached to the CIF file. The details of crystal parameters, data collection and refinements for **1** and **2** are listed in Table 1, and the selected bond lengths and angles are given in Table S1.

Adsorption equilibrium study. To explore the adsorption isotherms, 5 mg of **1** or **2** was added into 10 mL of CR solutions with different initial concentrations (10–200 mg L^{-1}) under neutral conditions. The mixture was stirred at 25 °C for 24 h, and the concentrations of the final CR solutions were determined by UV-vis spectroscopy after centrifugation. The equilibrium adsorption capacity q_e was calculated as:

$$q_e = (c_0\text{-}c_e)V/m$$

where c_0 and c_e (mg L^{-1}) are concentrations at the initial and equilibrium times. V (L) is the volume of the CR solution. m (mg) is the weight of the adsorbent.

Desorption and reusability study. Since the regeneration of the adsorbent is important in practical applications, the used adsorbent was washed with ethanol by ultrasonication and centrifugation several times and then dried in vacuum at 100 °C for 10 h.

Table S1. Selected bond lengths (Å) and angles (°) for **1** - **5**.

Compound **1**			
Cu(1)-O(1)	2.3416(14)	Cu(1)-O(2)	1.9458(12)
Cu(1)-N(1)#2	2.0239(14)		
O(1)-Cu(1)-O(2)	85.87(5)	O(1)-Cu(1)-O(2)#1	94.13(5)
O(1)-Cu(1)-N(1)#2	88.73(5)	O(1)-Cu(1)-N(1)#3	91.27(5)
O(2)-Cu(1)-N(1)#2	89.83(5)	O(2)-Cu(1)-N(1)#3	90.17(5)
Symmetry transformations used to generate equivalent atoms:			
#1 -x+5/3,-y+4/3,-z+1/3; #2 x-y+1,x,-z+1; #3 -x+y+2/3,-x+4/3,z-2/3			
Compound **2**			
Co(1)-O(1)	2.108(3)	Co(1)-O(2)	1.999(2)
Co(1)-N(1)#2	2.160(3)		
O(1)-Co(1)-O(2)#1	91.85(10)	O(1)-Co(1)-N(1)#2	90.07(11)
O(1)-Co(1)-N(1)#3	89.93(11)	O(2)-Co(1)-N(1)#2	91.26(11)
O(2)-Co(1)-N(1)#3	88.73(11)	O(1)-Co(1)-O(2)	88.15(10)
Symmetry transformations used to generate equivalent atoms:			
#1 -x+4/3,-y+5/3,-z+5/3; #2 y,-x+y+1,-z+1; #3 -y+4/3,x-y+2/3,z+2/3			
Compound **3**			
Zn(1)-O(1)	2.1156(16)	Zn(1)-O(2)	2.0458(14)
Zn(1)-N(1)#2	2.1661(17)	O(1)-Zn(1)-O(1)#1	179.63(8)
O(1)-Zn(1)-O(2)	88.54(6)	O(1)-Zn(1)-O(2)#1	91.20(6)
O(1)-Zn(1)-N(1)#2	87.32(6)	O(2)-Zn(1)-N(1)#3	89.25(7)
O(1)#1-Zn(1)-N(1)#2	92.93(7)	O(2)-Zn(1)-O(2)#1	89.79(9)
O(2)-Zn(1)-N(1)#2	175.73(6)	N(1)#2-Zn(1)-N(1)#3	92.01(10)
Symmetry transformations used to generate equivalent atoms:			
#1 -x+1,y,-z+1/2; #2 x+1/2,y+1/2,z; #3 -x+1/2,y+1/2,-z+1/2			
Compound **4**			
Co(1)-O(1)	2.1057(18)	Co(1)-O(2)	2.0073(17)
Co(1)-N(1)#2	2.183(2)		
O(1)-Co(1)-O(2)#1	92.24(7)	O(1)-Co(1)-N(1)#2	88.81(8)
O(1)-Co(1)-N(1)#3	91.19(8)	O(2)-Co(1)-N(1)#2	88.06(8)
O(2)-Co(1)-N(1)#3	91.94(8)	O(1)-Co(1)-O(2)	87.76(7)
Symmetry transformations used to generate equivalent atoms:			

#1 -x+1,-y+1,-z+1; #2 -x+3/2,y+1/2,-z+1/2; #3 x-1/2,-y+1/2,z+1/2

Compound **5**

Cu(1)-N(1)	2.052(3)	Cu(1)-I(1)	2.5965(6)
Cu(1)-I(1)#1	2.6170(5)	Cu(1)-I(1)#2	2.7434(6)
N(1)-Cu(1)-I(1)	109.94(9)	N(1)-Cu(1)-I(1)#1	110.37(9)
N(1)-Cu(1)-I(1)#2	97.78(9)	I(1)-Cu(1)-I(1)#1	120.51(2)
I(1)-Cu(1)-I(1)#2	115.903(19)	I(1)#1-Cu(1)-I(1)#2	99.730(19)

Symmetry transformations used to generate equivalent atoms:

#1 -x+1,y-1/2,-z+1/2; #2 -x+1,y+1/2,-z+1/2

Table S2. Hydrogen bonding data of **5**.

D–H···A	d(*D*–H) (Å)	d(H···A) (Å)	d(*D*···A)(Å)	*D*–H···A (°)
C(10)-H(10)···O(2)	0.95	2.63	3.37	135
C(6)-H(6)···I(1)	0.95	3.18	3.82	127

Table S3. Detection limit for NZF using different MOFs.

MOF	Detection limit (ppb)	Ref.
3	240	This work
$[Cd(L)_{0.5}(bpda)]\cdot 1.5DMF\cdot 0.5H_2O$	252	S5
$[Zn(L)_{0.5}(NDC)_{0.5}(HCOO)]\cdot H_2O$	184	S6
$[NaEu_2(TATAB)_2(DMF)_3]OH$	441	S7
$(Me_2NH_2)[In(BCP)]\cdot 2.5DEF$	282	S8

L= 3,3',5,5'-tetra(1H-imidazol-1-yl)biphenyl,

H_2bpda = 4,4'-carbonyldibenzoic acid,

H_2NDC = 2,6-naphthalenedicarboxylic acid,

H_3TATAB = 4,4',4''-*s*-triazine-1,3,5-triyltri-*m*-aminobenzoic acid,

H_4BCP = 5-(2,6-bis(4-carboxyphenyl) pyridin-4-yl) isophthalic acid.

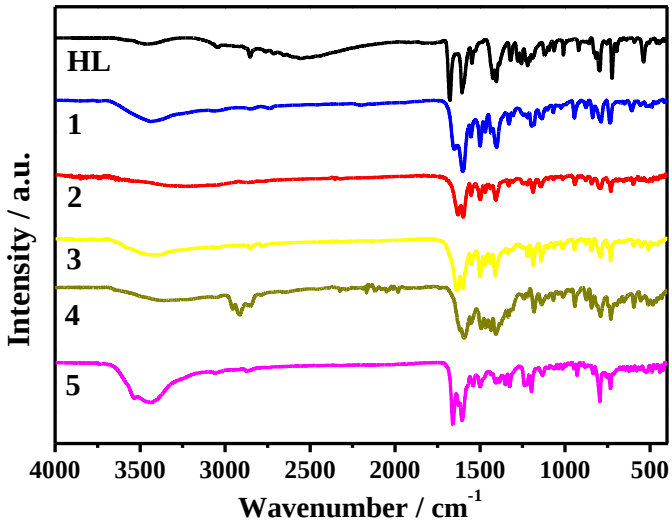

Fig. S1. IR spectra of HL, **1 - 5**.

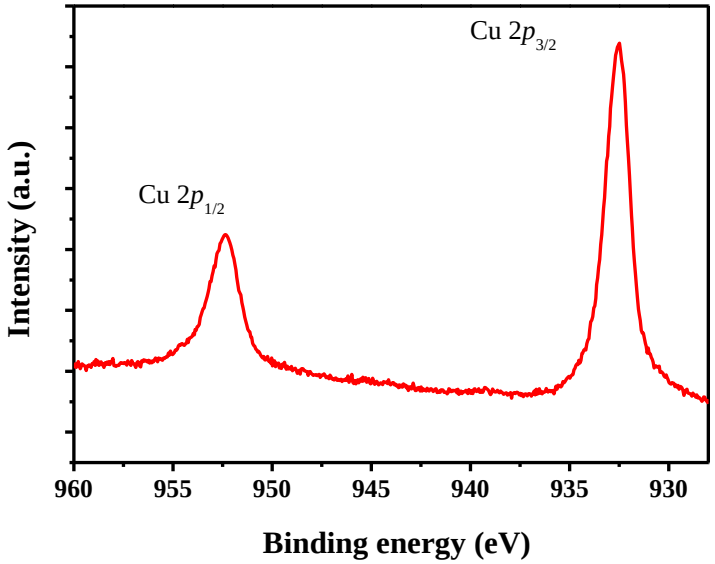

Fig. S2. Cu 2p XPS spectrum of **5**.

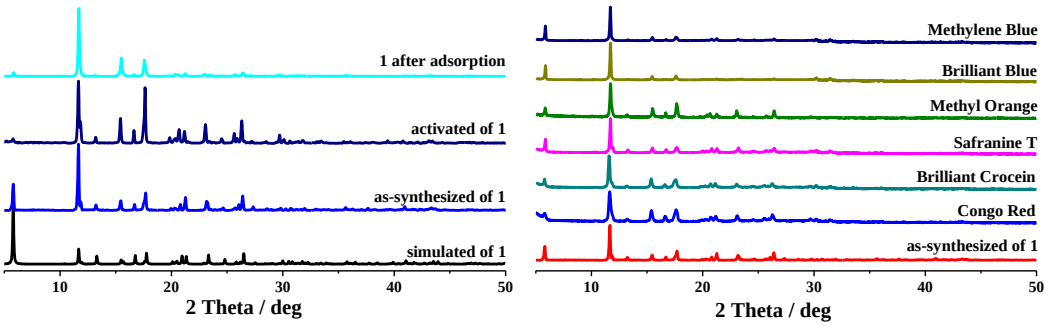

(a) **(b)**

Fig. S3. PXRD patterns of **1** (a) simulated, as-synthesized, activated, after gas adsorption measurements and (b) after adsorption of dyes.

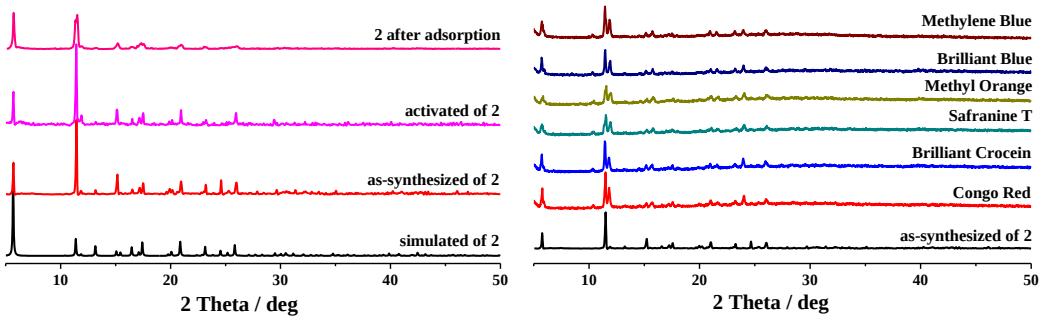

(a) **(b)**

Fig. S4. PXRD patterns of **2** (a) simulated, as-synthesized, activated, after gas adsorption measurements and (b) after adsorption of dyes.

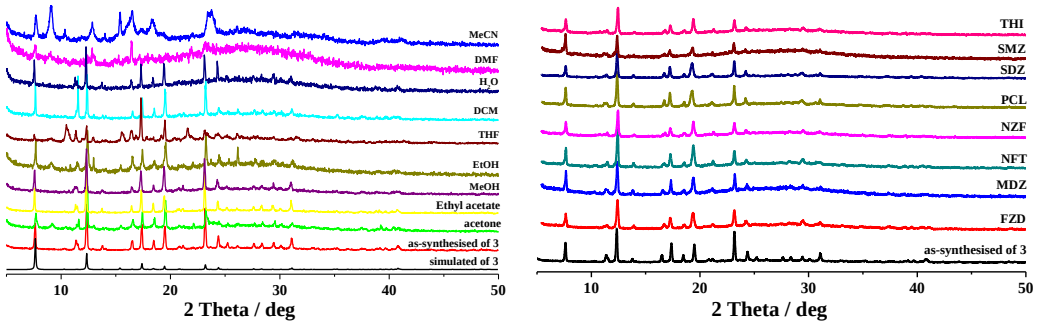

(a) **(b)**

Fig. S5. PXRD patterns of **3** (a) simulated, as-synthesized **3**, in different solvent for 10 h and (b) after detecting antibiotics.

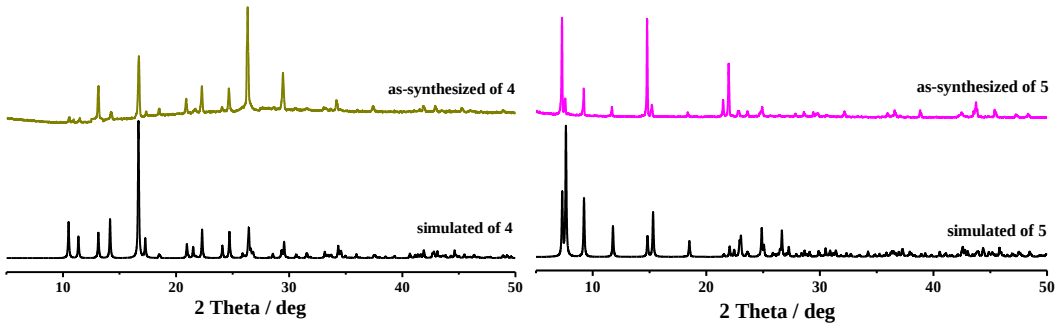

(a) **(b)**

Fig. S6. PXRD patterns of (a) simulated **4**, as-synthesized **4** and (b) simulated **5**, as-synthesized **5**.

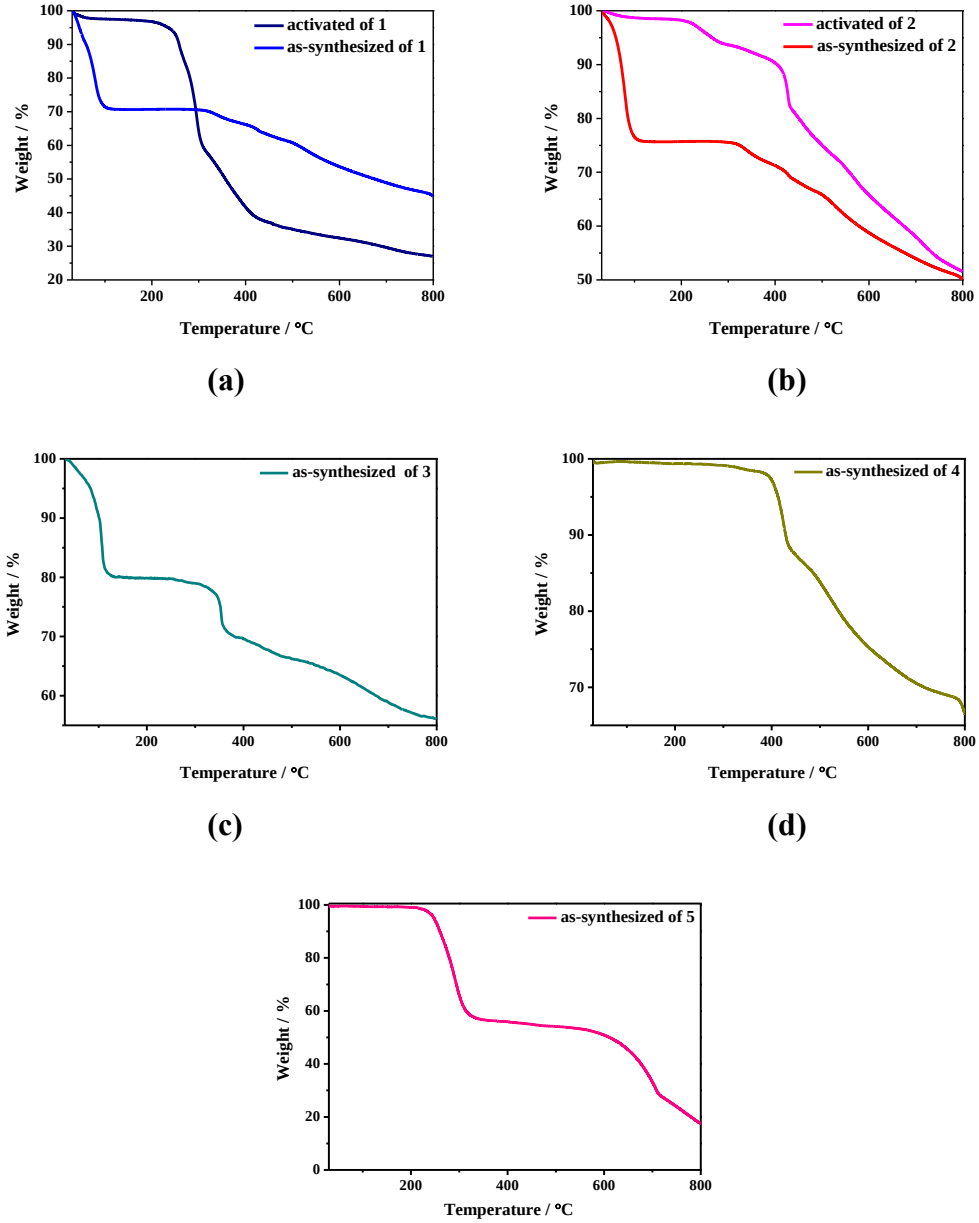

Fig. S7. TG curves of (a) **1**, the activated **1**, (b) **2** and the activated **2**, (c) **3**, (d) **4**, (e) **5**.

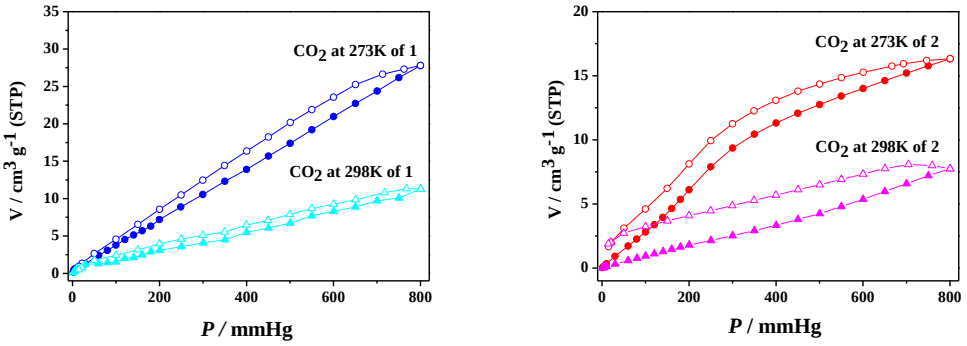

(a) **(b)**

Fig. S8. Adsorption and desorption isotherms of (a) **1** and (b) **2** at 273 K and 298K. Filled symbols = adsorption; empty symbols = desorption.

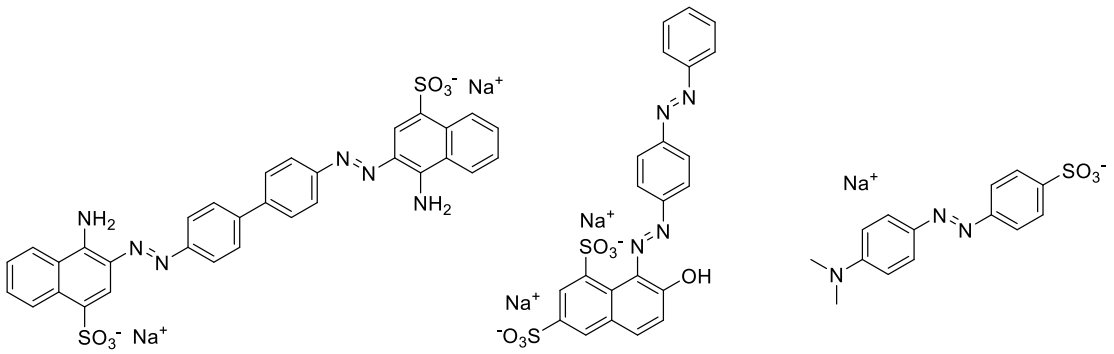

CR (2.47nm x1.23nm x1.25nm) BC (1.65nm x0.89nm x0.43nm) MO (1.45nm x0.43nm x0.31nm)

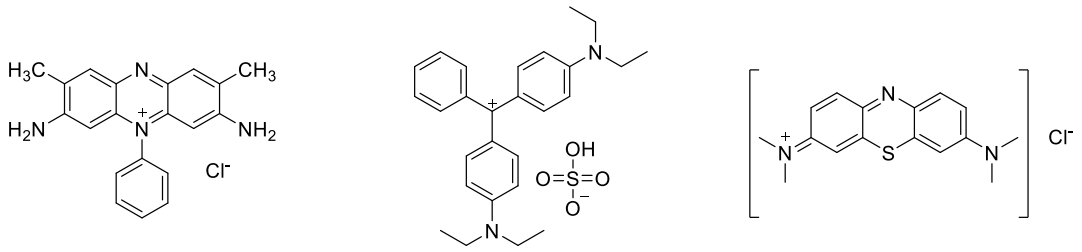

ST (1.18nm x0.95nm x0.46nm) BG (1.59nm x1.04nm x0.36nm) MEB (1.34nm x0.50nm x0.42nm)

Fig. S9. Structures and sizes of different dyes.

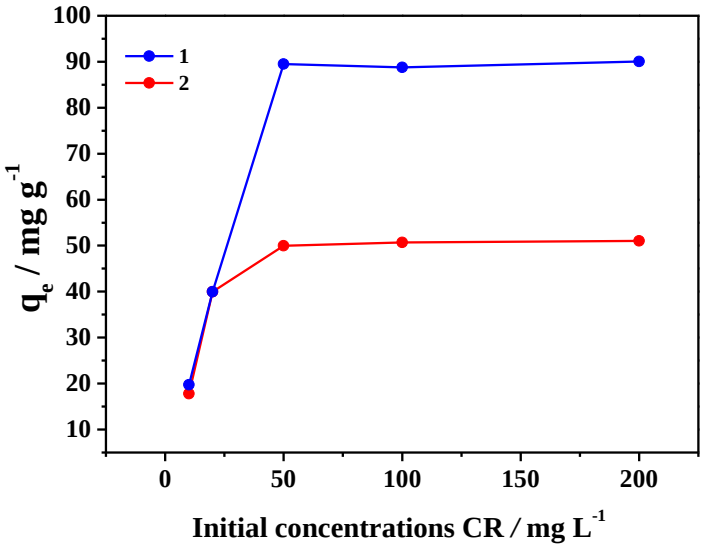

Fig. S10. Adsorption uptakes of **1** and **2** at different initial concentrations of CR solutions.

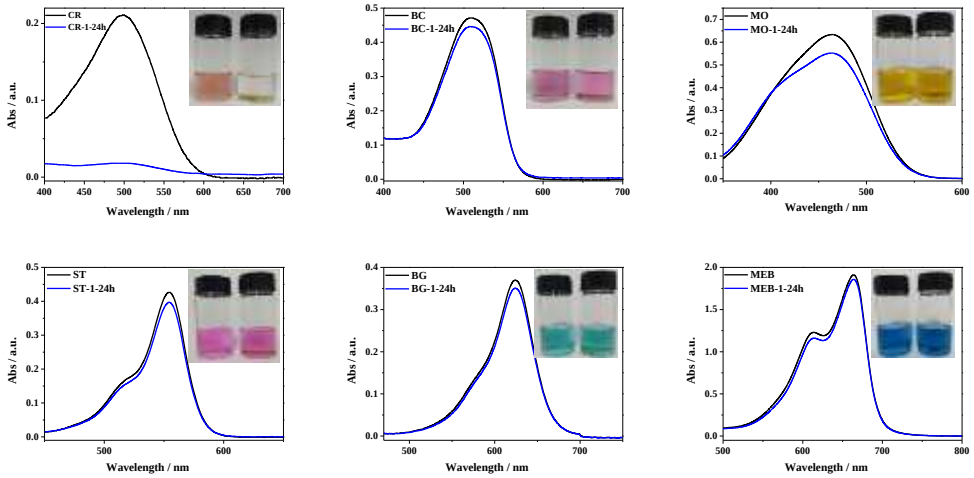

Fig. S11. Adsorption capability of **1** toward different dyes in an aqueous solution.

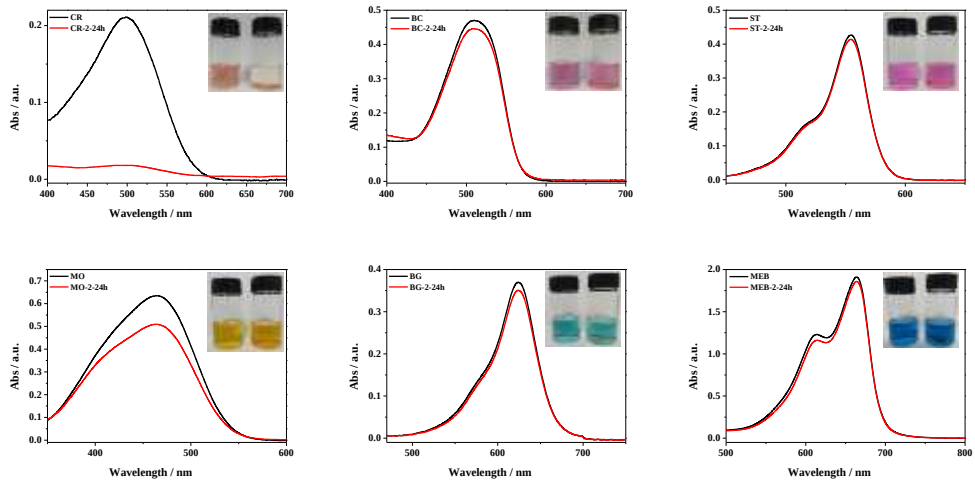

Fig. S12. Adsorption capability of **2** toward different dyes in an aqueous solution.

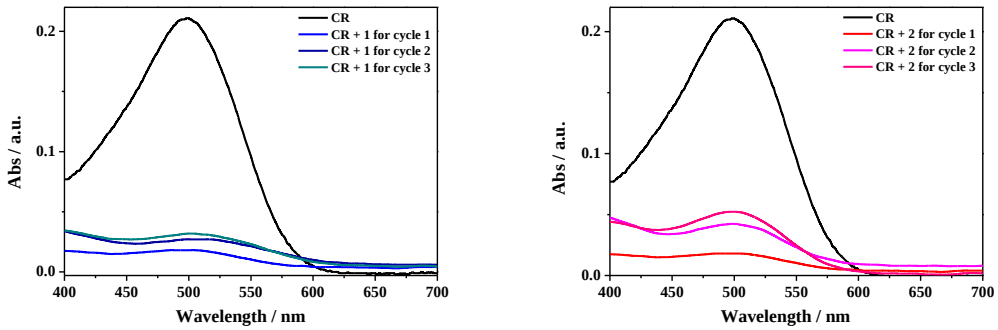

Fig. S13. Recycling adsorption ability of **1** and **2**.

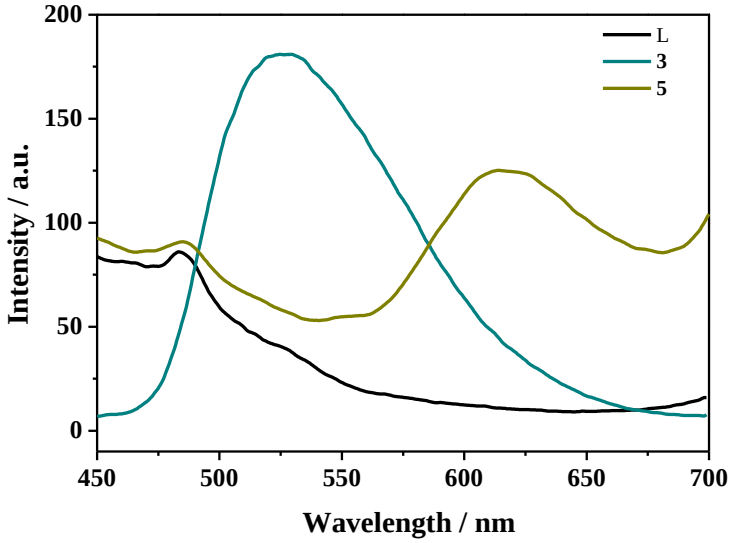

Fig. S14. Photoluminescence spectra of HL, **3** and **5** in the solid phase.

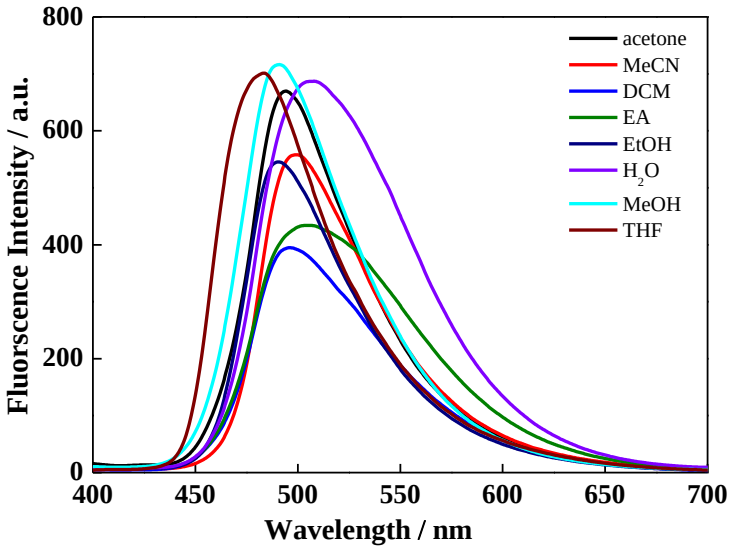

Fig. S15. The fluorescence spectra of **3** dispersed in different solvents excited at 370 nm.

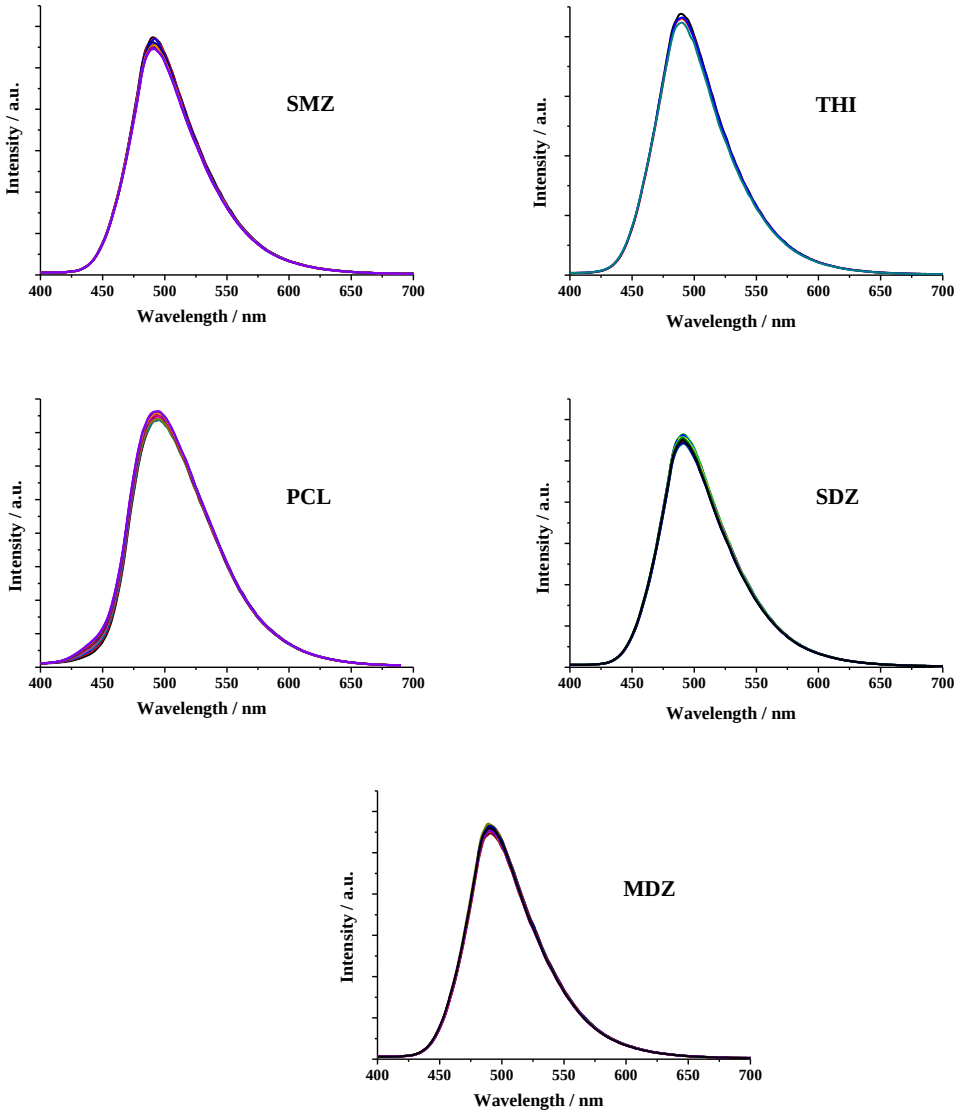

Fig. S16. The fluorescence spectra of **3** introduced into different antibiotics in MeOH excited at 370 nm.

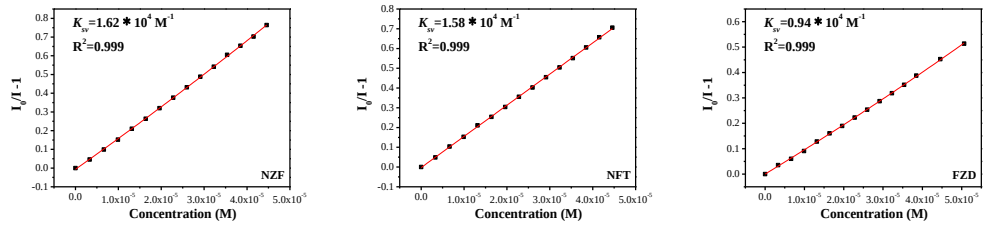

Fig. S17. Stern–Volmer plot of **3** for NZF, NFT and FZD, respectively.

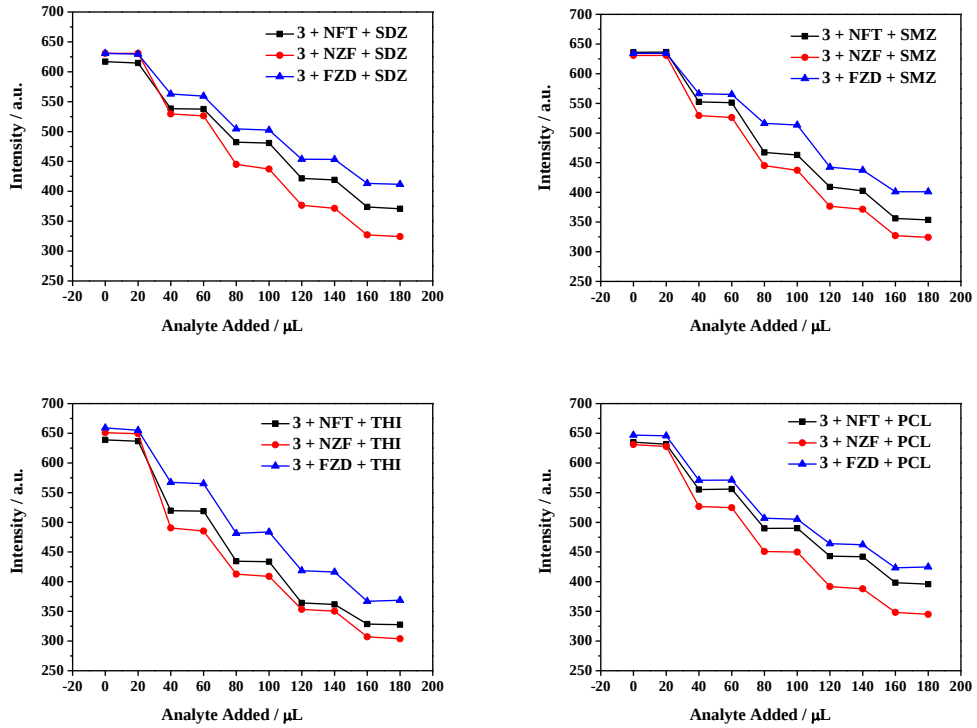

Fig. S18. Fluorescence quenching of **3** upon addition of NZF, NFT and FZD solution followed by SDZ, SMZ, THI and PCL, respectively.

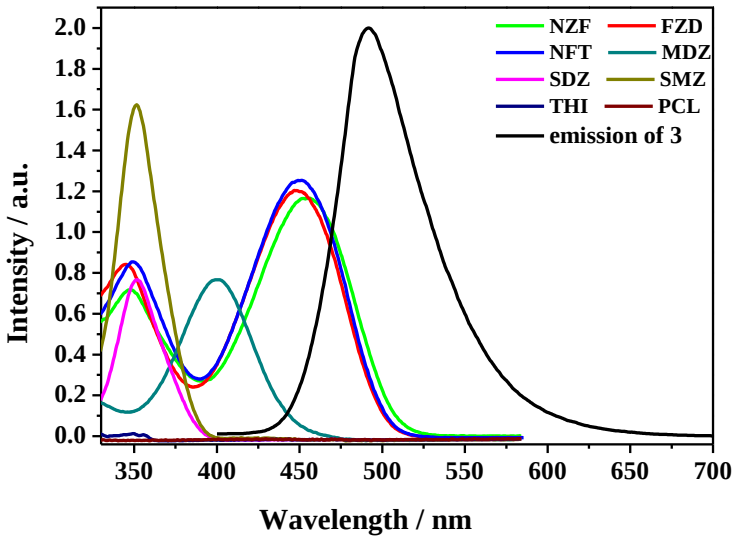

Fig. S19. Spectral overlap between the absorption of antibiotics and the emission of **3**.

Reference

(S1) G. M. Sheldrick, *SADABS*, *Program for Empirical Adsorption Correction of Area Detector Data*, University of Göttingen, Germany, 2003.

(S2) G. M. Sheldrick, *SHELXS-2014*, *Program for the Crystal Structure Solution,* University of Göttingen, Germany, 2014.

(S3) G. M. Sheldrick, *SHELXL-2018, Program for the Crystal Structure Refinement,* University of Göttingen, Germany, 2018.

(S4) P. van der Sluis, A. L. Spek, *Acta Crystallogr., Sect. A: Found. Crystallogr.* 1990, **46**, 194-201

(S5) Y. L. Xu, Y. Liu, X. H. Liu, Y. Zhao, P. Wang, Z. L. Wang and W. Y. Sun, *Polyhedron*, 2018, **154**, 350-356.

(S6) Y. L. Xu, Y. Liu, X. H. Liu, Y. Zhao, P. Wang, Z. L. Wang and W. Y. Sun, *Isr. J. Chem.*, 2019, **59**, 267-272.

(S7) M. L. Han, G. X. Wen, W. W. Dong, Z. H. Zhou, Y. P. Wu, J. Zhao, D. S. Li, L. F. Ma and X. Bu, *J. Mater. Chem. C*, 2017, **5**, 8469-8474.

(S8) S.L. Hou, J. Dong, X.L. Jiang, Z.H. Jiao, C.M. Wang, B. Zhao, Interpenetration-dependent luminescent probe in indium-organic frameworks for selectively detecting nitrofurazone in water. Anal. Chem. 90(2018) 1516-1519.